



UDC 669.168

DOI 10.17073/0368-0797-2023-6-743-749



Original article

Оригинальная статья

INFLUENCE OF BASICITY ON PHYSICAL PROPERTIES OF SLAGS OF THE $\text{CaO} - \text{SiO}_2 - 18\% \text{Cr}_2\text{O}_3 - 6\% \text{B}_2\text{O}_3 - 3\% \text{Al}_2\text{O}_3 - 8\% \text{MgO}$ SYSTEM

A. A. Babenko, R. R. Shartdinov[✉], A. G. Upolovnikova,
A. N. Smetannikov, D. A. Lobanov, A. V. Dolmatov

Institute of Metallurgy, Ural Branch of the Russian Academy of Sciences (101 Amundsen Str., Yekaterinburg 620016, Russian Federation)

✉ rr.shartdinov@gmail.com

Abstract. Influence of basicity on viscosity, crystallization onset temperature, phase composition, and structure of slags of the $\text{CaO} - \text{SiO}_2 - 18\% \text{Cr}_2\text{O}_3 - 6\% \text{B}_2\text{O}_3 - 3\% \text{Al}_2\text{O}_3 - 8\% \text{MgO}$ system in the basicity range ($B = \text{CaO}/\text{SiO}_2$) from 1.0 up to 2.5 was studied using vibrational viscometry, thermodynamic modeling, and Raman spectroscopy. It was established that the physical properties of slags depend on the balance of polymerization degree and phase composition. Acid slags with a basicity of 1.0 belong to the category of “long” slags and are characterized by an increased proportion of high-temperature phases up to 34.1 %. However, despite the fact that the proportion of high-temperature phases is 1.6 times higher compared to the proportion of low-temperature ones, they are characterized by a simpler silicate structure, providing a viscosity of no more than 0.25 Pa·s at a crystallization onset temperature of 1530 °C. An increase in basicity of slags of the studied oxide system (up to 2.5), along with an increase in the proportion of high-temperature phases (by almost 5.9 times), is accompanied by formation of a more complex silicate structure. The resulting four-coordination structural elements $[\text{CrO}_4]$ and $[\text{AlO}_4]$ are embedded in the silicate structure and complicate it, which increases the polymerization degree. Thus, at basicity of 2.5, due to a high proportion of high-temperature phases in the slag and development of polymerization process, slag crystallization onset temperature increases to 1700 °C and its viscosity reaches 1.0 Pa·s at a temperature of 1670 °C.

Keywords: AOD-slag, boron oxide, chromium oxide, structure, viscosity, phase composition, crystallization onset temperature

Acknowledgements: The work was performed according to the state assignment of the Institute of Metallurgy, Ural Branch of the Russian Academy of Sciences using the equipment of the Shared Access Center “Composition of Compounds” of Institute of High Temperature Electronics, Ural Branch of the Russian Academy of Sciences.

For citation: Babenko A.A., Shartdinov R.R., Upolovnikova A.G., Smetannikov A.N., Lobanov D.A., Dolmatov A.V. Influence of basicity on physical properties of slags of the $\text{CaO} - \text{SiO}_2 - 18\% \text{Cr}_2\text{O}_3 - 6\% \text{B}_2\text{O}_3 - 3\% \text{Al}_2\text{O}_3 - 8\% \text{MgO}$ system. *Izvestiya. Ferrous Metallurgy*. 2023;66(6): 743–749.
<https://doi.org/10.17073/0368-0797-2023-6-743-749>

ВЛИЯНИЕ ОСНОВНОСТИ НА ФИЗИЧЕСКИЕ СВОЙСТВА ШЛАКОВ СИСТЕМЫ $\text{CaO} - \text{SiO}_2 - 18\% \text{Cr}_2\text{O}_3 - 6\% \text{B}_2\text{O}_3 - 3\% \text{Al}_2\text{O}_3 - 8\% \text{MgO}$

А. А. Бабенко, Р. Р. Шартдинов[✉], А. Г. Уполовникова,
А. Н. Сметанников, Д. А. Лобанов, А. В. Долматов

Институт metallurgии Уральского отделения РАН (Россия, 620016, Свердловская обл., Екатеринбург, ул. Амудсена, 101)

✉ rr.shartdinov@gmail.com

Аннотация. В работе исследовано влияние основности на вязкость, температуру начала кристаллизации, фазовый состав и структуру шлаков системы $\text{CaO} - \text{SiO}_2 - 18\% \text{Cr}_2\text{O}_3 - 6\% \text{B}_2\text{O}_3 - 3\% \text{Al}_2\text{O}_3 - 8\% \text{MgO}$ в диапазоне основности от 1,0 до 2,5 методами вибрационной вискозиметрии, термодинамического моделирования и рамановской спектроскопии. Физические свойства шлаков зависят от баланса процессов полимеризации и формирования фазового состава. Кислые шлаки основностью 1,0 относятся к категории «длинных» шлаков и характеризуются повышенной (до 34,1 %) долей высокотемпературных фаз. Однако, несмотря на то, что доля высокотемпературных фаз в 1,6 раза выше по сравнению с долей низкотемпературных фаз, они характеризуются более простой силикатной структурой, обеспе-

чивая при температуре начала кристаллизации 1530 °C вязкость не более 0,25 Па·с. Рост основности (до 2,5) шлаков изучаемой оксидной системы, наряду с повышением (примерно в 5,9 раза) доли высокотемпературных фаз, сопровождается формированием более сложной силикатной структуры. Образующиеся четырехкоординационные структурные элементы $[CrO_4]$ и $[AlO_4]$ встраиваются в кремний-кислородную решетку и усложняют ее, что повышает степень полимеризации. Таким образом, при основности 2,5, в связи с высокой долей высокотемпературных фаз в шлаке и развитием процесса полимеризации, температура начала кристаллизации шлака возрастает до 1700 °C, а его вязкость достигает 1,0 Па·с при температуре 1670 °C.

Ключевые слова: АКР-шлак, оксид бора, оксид хрома, структура, вязкость, фазовый состав, температура начала кристаллизации

Благодарности: Работа выполнена по государственному заданию Института металлургии Уральского отделения РАН с использованием оборудования ЦКП «Состав вещества» Института высокотемпературной электрохимии Уральского отделения РАН.

Для цитирования: Бабенко А.А., Шартдинов Р.Р., Уполовникова А.Г., Сметанников А.Н., Лобанов Д.А., Долматов А.В. Влияние основности на физические свойства шлаков системы $CaO - SiO_2 - 18\% Cr_2O_3 - 6\% B_2O_3 - 3\% Al_2O_3 - 8\% MgO$. Известия вузов. Черная металлургия. 2023;66(6):743–749. <https://doi.org/10.17073/0368-0797-2023-6-743-749>

INTRODUCTION

In the contemporary field of low-carbon stainless steel production, argon-oxygen decarburization (AOD) technology predominates, entailing phases of oxidation and reduction. The reduction phase slags, rich in chromium oxide, present significant challenges in chromium reduction and steel desulfurization due to their high viscosity and refractory nature. To mitigate these issues, calcium fluoride is traditionally added as a fluxing agent during the reduction phase [1]. However, this addition poses drawbacks, including aggressive wear on the refractory lining, alterations in slag composition over time, and the formation of environmentally detrimental volatile fluorides [2]. Therefore, researchers have to find a way to replace it. One of the solutions can be the use of boron oxide. In response to these challenges, boron oxide emerges as a promising alternative, attributed to its beneficial impact on slag viscosity and crystallization temperature [3 – 5]. Nonetheless, the specific influence of boron oxide on the physical properties of chromium-containing slags remains largely underexplored.

This study employs vibrational viscometry, thermodynamic modeling of phase composition (HSC Chemistry 6.12 (Outokumpu)), and Raman spectroscopy to investigate the effects of varying basicity ($B = CaO/SiO_2$) from 1.0 to 2.5 – mirroring the composition at the commencement of the AOD process reduction period – on the viscosity η , crystallization onset temperature (t_{cr}), phase composition and structure of slags in the $CaO - SiO_2 - 18\% Cr_2O_3 - 6\% B_2O_3 - 3\% Al_2O_3 - 8\% MgO$ system [6].

MATERIALS AND METHODS

To study the physical properties of slags within the six-component oxide system $CaO - SiO_2 - 18\% Cr_2O_3 - 6\% B_2O_3 - 3\% Al_2O_3 - 8\% MgO$, experimental slags were synthesized with compositions detailed in Table 1.

These slags were produced in a resistance furnace using molybdenum crucibles under an argon atmosphere, employing analytical-reagent grade oxides pre-calculated at 800 °C (with B_2O_3 calcinated at 100 °C) for 2 to 3 h.

The viscosity measurements for these slags were conducted utilizing a vibrating viscometer [7] within molybdenum crucibles in an argon flow, with temperature monitoring achieved through a tungsten-rhenium thermocouple. The slags' crystallization onset temperatures were ascertained based on Frenkel's theory of viscous flow. This involved plotting graphs in the coordinates $\ln \eta - 1/T$, with the crystallization temperature identified at the inflection point of these curves [8].

Thermodynamic modeling of the phase composition for the experimental slag samples was performed using the HSC Chemistry 6.12 software package (Outokumpu) [9].

The structure of slag samples was investigated using a Raman microscope spectrometer (U 1000) quipped with a 532 nm excitation wavelength laser. The acquired spectra span a wave number range of 200 to 1600 cm^{-1} . The spectrum lines observed can be unequivocally linked to the vibrational movements of the molecules within the slag sample. An analysis of the slag's structure is facilitated through examination of the oscillation frequency, as well as the intensity and contour of these spectrum lines [10].

RESULTS AND DISCUSSION

Fig. 1 illustrates the relationship between slag viscosity, temperature, and basicity. Fig. 2 presents these relationships

Table 1

Composition of experimental slags

Таблица 1. Состав экспериментальных шлаков

Slag	Content, %						B	t_{cr} , °C
	CaO	SiO ₂	Cr ₂ O ₃	MgO	Al ₂ O ₃	B ₂ O ₃		
1	32.5	32.5	18.0	8.0	3.0	6.0	1.0	1530
2	39.0	26.0	18.0	8.0	3.0	6.0	1.5	1552
3	43.3	21.7	18.0	8.0	3.0	6.0	2.0	1614
4	46.4	18.6	18.0	8.0	3.0	6.0	2.5	1700

within the coordinates $\ln \eta - 1/T$, facilitating the determination of the crystallization temperature (Table 1).

Table 2 outlines the phase composition modeling results for the slag samples tested. Based on their melting temperatures, all phases have been categorically divided into three groups: low-temperature ($1130 - 1280$ °C), medium-temperature ($1460 - 1600$ °C), and high-temperature ($1710 - 2852$ °C).

Raman spectroscopy results of the experimental slag samples, with basicities of 1.0 and 2.5 (slags 1 and 4, respectively) and a constant content of chromium oxide (18 %) and boron oxide (6.0 %), are depicted in Fig. 3. Table 3 correlates the wave numbers to the peaks of structural elements observed.

Peaks within the wave number ranges of 470 to 660 and 250 to 400 cm⁻¹ are associated with symmetric stretching and bending vibrations of Si–O–Si linkages. Peaks at 550 cm⁻¹, found within these ranges, are attributed to Al–O–Al and Cr–O–Cr connections. As slag basicity increases, these peaks, including the Si–O–Si linkages, become less distinct.

Variations in the wave number region of 800 to 1200 cm⁻¹ indicate that with an increase in basicity to 2.5, Raman spectrum peaks corresponding to [CrO₄] and Q_{Al}³ appear at wave numbers 873 and 780 cm⁻¹. This suggests the presence of these structural components in slags with elevated basicity, recognized as slag polymerizers [14; 19].

Fig. 3 lacks peaks corresponding to three-coordination boron [BO₃], indicating that within the slag structure, boron oxide is represented by four-coordination boron [BO₄]. The [BO₄] tetrahedra tend to create bonds with silicon atoms, complicating the structure, but at the same time, reducing its uniformity and strength [20 – 22]. Reduction in the slag viscosity when such oxide is used as a fluxing agent can be attributed to weakening of the structure and formation of low-melting compounds.

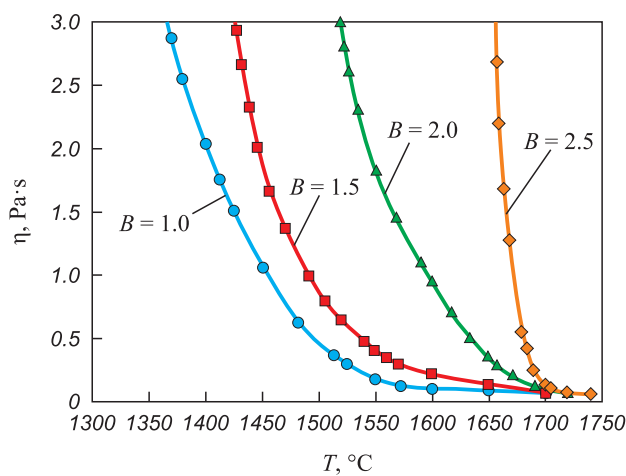


Fig. 1. Dependence of viscosity on temperature and basicity of slags of the studied oxide system

Рис. 1. Зависимость вязкости от температуры и основности шлаков изучаемой оксидной системы

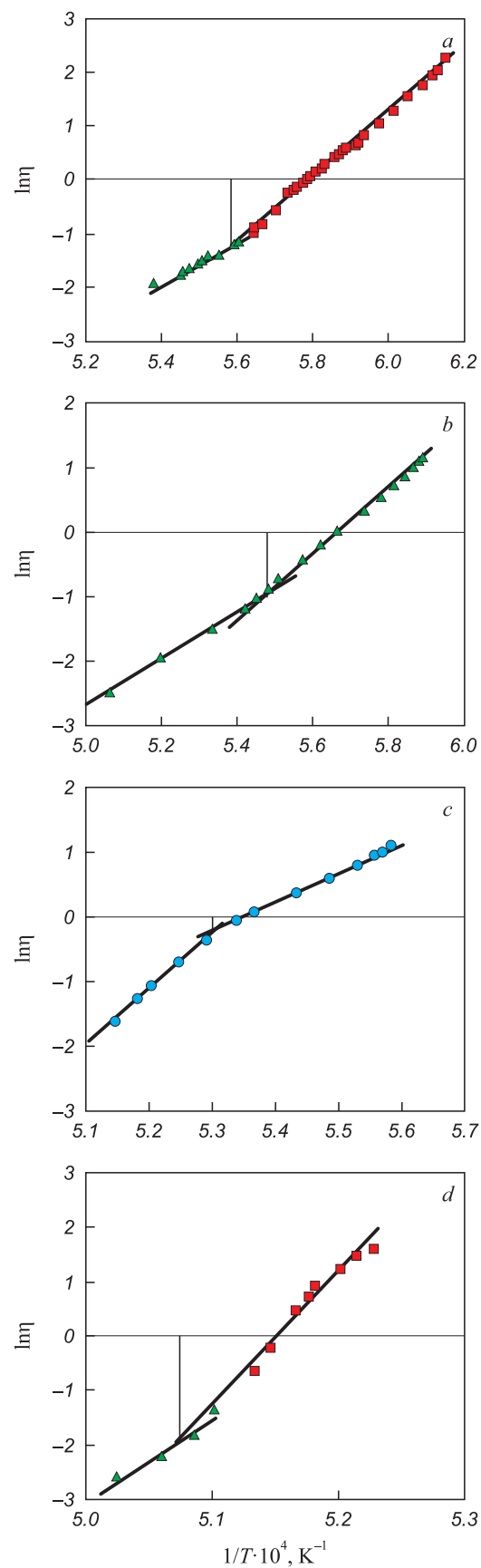


Fig. 2. Dependence of viscosity logarithm of (ln η) on inverse absolute temperature (1/T) for slags 1 – 4 (a – d)

Рис. 2. Зависимость логарифма вязкости (ln η) от обратной абсолютной температуры (1/T) шлаков 1 – 4 (a – d)

Table 2

Phase composition of experimental slags at 1600 °C

Таблица 2. Фазовый состав экспериментальных шлаков при 1600 °C

Phase composition	Melting temperature, °C	Content, %, in the slag			
		1	2	3	4
Low-temperature phases					
CB	1130	4.3	2.8	1.4	0.4
2CB	1280	8.3	10.1	10.7	8.4
CM2S	1391	9.2	5.6	2.0	0.3
Total		21.8	18.5	14.1	9.1
Medium-temperature phases					
2CM2S	1454	3.0	3.4	2.7	1.0
3CB	1460	0.7	1.7	3.9	8.9
3C2S	1460	5.6	7.5	8.1	6.0
CMS	1503	7.7	9.9	10.9	8.4
CS	1540	15.9	13.1	9.0	4.6
CA2S	1550	3.6	1.8	0.4	0.02
MS	1557	5.8	4.0	2.0	0.5
3CM2S	1575	1.2	2.5	4.3	4.9
CA	1600	0.4	0.9	1.9	3.2
Total		43.9	44.8	43.2	37.52
High-temperature phases					
S	1710	4.9	2.2	0.7	0.1
A	2040	1.4	1.8	1.7	1.0
2CS	2130	6.3	9.6	14.6	21.9
C	2570	0.2	0.4	0.7	2.2
M	2852	1.4	2.0	3.1	4.8
Cr	2435	12.8	10.3	6.8	3.0
CCr	2100	7.1	10.6	15.4	20.5
Total		34.1	36.9	43.0	53.5

Note (phase designations):

CB – $\text{CaO}\cdot\text{B}_2\text{O}_3$; 2CB – $2\text{CaO}\cdot\text{B}_2\text{O}_3$;
 3CB – $3\text{CaO}\cdot\text{B}_2\text{O}_3$; CS – $\text{CaO}\cdot\text{SiO}_2$; 2CS – $2\text{CaO}\cdot\text{SiO}_2$;
 3C2S – $3\text{CaO}\cdot2\text{SiO}_2$; C – CaO ; CM2S – $\text{CaO}\cdot\text{MgO}\cdot2\text{SiO}_2$;
 CMS – $\text{CaO}\cdot\text{MgO}\cdot\text{SiO}_2$; 2CM2S – $2\text{CaO}\cdot\text{MgO}\cdot2\text{SiO}_2$;
 3CM2S – $3\text{CaO}\cdot\text{MgO}\cdot2\text{SiO}_2$; S – SiO_2 ; MS – $\text{MgO}\cdot\text{SiO}_2$;
 M – MgO ; CA2S – $\text{CaO}\cdot\text{Al}_2\text{O}_3\cdot2\text{SiO}_2$; A – Al_2O_3 ;
 CA – $\text{CaO}\cdot\text{Al}_2\text{O}_3$; Cr – Cr_2O_3 ; CCr – $\text{CaO}\cdot\text{Cr}_2\text{O}_3$.

The polymerization degree of slag is primarily influenced by the high-frequency silicate region, spanning wave numbers 800 to 1200 cm^{-1} , which correspond to $[\text{SiO}_4]$ tetrahedrons. To gain a more nuanced understanding of the slag's structural intricacies, we performed deconvolution of the obtained Raman spectra using the Gaussian method [23] (Fig. 4). This process facilitated the representation of the slag's polymerization degree through the quantification of the average number of bridging oxygen (BO) molecules, calculated by the formula:

$$\text{BO} = 0 \cdot Q_{\text{Si}}^0 + 1 \cdot Q_{\text{Si}}^1 + 2 \cdot Q_{\text{Si}}^2 + 3 \cdot Q_{\text{Si}}^3 + 4 \cdot Q_{\text{Si}}^4, \quad (1)$$

where Q_{Si}^n is $[\text{SiO}_4]$ with n number of bridging oxygen.

Calculations of the average amount of bridging oxygen (BO) are presented in Table 4.

Acid slags with a basicity of 1.0 (Fig. 1, slag 1) categorized as “long” slags, are shown to possess a heightened proportion of high-temperature phases, reaching up to 34.1 % (Table 2). However, despite the fact that the proportion of high-temperature phases is 1.6 times higher compared to that of low-temperature phases, slags with a basicity of 1.0 have a simpler silicate structure. The average amount of bridging oxygen BO does not exceed 0.55, likely because chromium oxide behaves more like a base in the acidic slag environment [24; 25]. The depolymerizing impact on the silicon-oxygen lattice results in a majority (0.64) of the silicate structural elements being composed of $[\text{SiO}_4]$ units devoid of bridging oxygen. This simpler structure, particularly in slags with a basicity of 1.0, ensures relatively high fluidity at a crystallization temperature of 1530 °C, despite having a 1.6-fold greater proportion of high-temperature phases. At and above the crystallization temperature, the viscosity of the slag remains below 0.25 Pa·s.

Table 3

Correspondence of wave numbers and structures

Таблица 3. Соответствие волновых чисел и структур

Elements	Wave number, cm^{-1}	Structures	References
Q_{Si}^0	850 – 880	without bridging oxygen in $[\text{SiO}_4]$	[11; 12]
Q_{Si}^1	900 – 920	with 1 bridging oxygen in $[\text{SiO}_4]$	
Q_{Si}^2	950 – 980	with 2 bridging oxygen in $[\text{SiO}_4]$	
Q_{Si}^3	1040 – 1060	with 3 bridging oxygen in $[\text{SiO}_4]$	
Q_{Si}^4	1060, 1190	with 4 bridging oxygen in $[\text{SiO}_4]$	
Si–O–Si	500 – 650	deformation vibrations Si – O ⁰	[13]
Al–O–Al	550	stretch vibrations Al – O ⁰	[14]
Cr–O–Cr	520 – 540	stretch vibrations Cr – O ⁰	[15]
[CrO ₄]	873	stretch vibrations Cr – O ⁰	[16]
[BO ₃]	1350 – 1530	stretch vibrations B – O ⁻ in $[\text{BO}_3]^-$	[17; 18]
[BO ₄]	900 – 920	stretch vibrations B – O ⁰ in $[\text{BO}_4]$	[18]
Q_{Al}^3	780	with 3 bridging oxygen in $[\text{AlO}_4]$	[14]

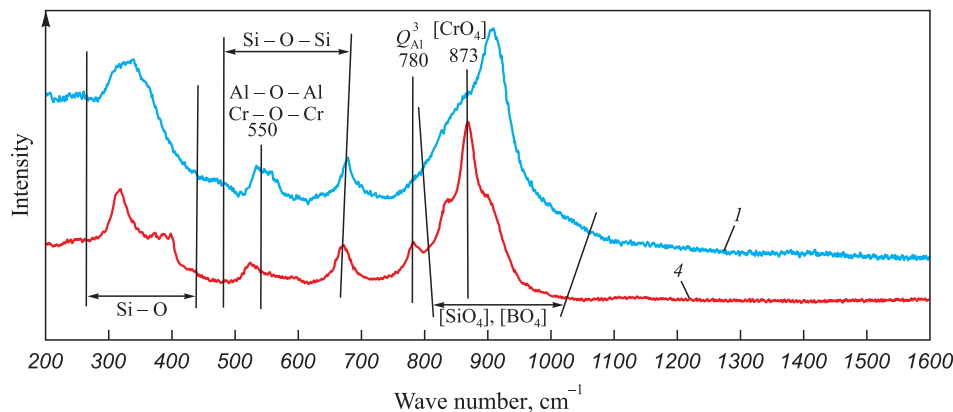


Fig. 3. Raman spectra of slags I and 4

Рис. 3. Рамановские спектры шлаков I и 4

As the basicity of the slags within this oxide system increases, the trend of a rising proportion of high-temperature phases and a declining proportion of low-temperature ones continues (as indicated in Table 2). For instance, a slag with a basicity of 2.5 (slag 4, Fig. 1) is classified as belonging to the “short” slags category (Table 2), with its high-

temperature phase proportion escalating to 53.5 %. This increase is largely attributable to the phases $2\text{CaO}\cdot\text{SiO}_2$ (21.9 %) and $\text{CaO}\cdot\text{Cr}_2\text{O}_3$ (20.5 %), alongside a reduction in low-temperature phases to 9.1 %, due to diminished proportions of $\text{CaO}\cdot\text{B}_2\text{O}_3$ and $\text{CaO}\cdot\text{MgO}\cdot2\text{SiO}_2$ to 0.4 and 0.3 %, respectively. Concurrently, despite the enhanced basicity and the integration of the $[\text{BO}_4]$ structural element, the presence of chromium and aluminum oxides, acting as acidic oxides [14; 19; 20], leads to a heightened polymerization degree of the slag. The incorporation of four-coordination chromium $[\text{CrO}_4]$ and aluminum $[\text{AlO}_4]$ into the silicon-oxygen framework intensifies its complexity. Consequently, the average number of bridging oxygen (BO) rises to 0.73, predominantly because a significant portion (0.52) of the silicate structural elements consists of $[\text{SiO}_4]$ with one bridging oxygen. This intricate silicate structure, alongside an approximately 5.9-fold increase in the proportion of high-temperature phases compared to low-temperature ones, contributes to a rise in the crystallization temperature to 1700 °C and viscosity levels reaching 1.0 Pa·s or more at temperatures of 1670 °C and below.

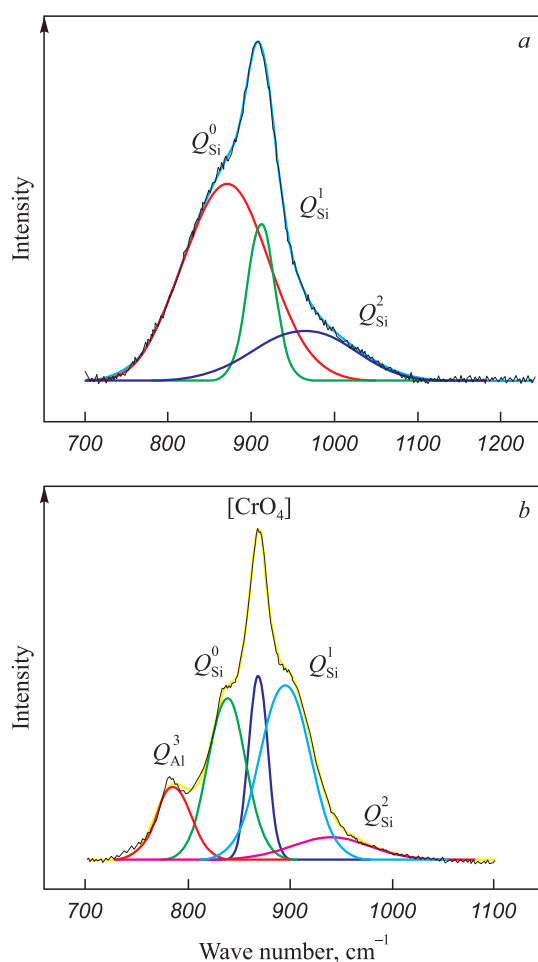


Fig. 4. Results of deconvolution of slags I (a) and 4 (b)

Рис. 4. Результаты деконволюции шлаков I (а) и 4 (б)

CONCLUSIONS

Our research has revealed new details about how the basicity of slags in the $\text{CaO}-\text{SiO}_2-18\% \text{Cr}_2\text{O}_3-$

Table 4

Fractions of silicate structural elements

Таблица 4. Количество силикатных структурных элементов

Slag	B	Number of structural elements, shares				BO
		Q_{Si}^0	Q_{Si}^1	Q_{Si}^2	Q_{Si}^3	
I	1.0	0.64	0.17	0.19	0	0.55
4	2.5	0.37	0.52	0.11	0	0.73

$-6\% \text{B}_2\text{O}_3 - 3\% \text{Al}_2\text{O}_3 - 8\% \text{MgO}$ system impacts their phase composition, structure, viscosity, and the temperature at which they begin to crystallize.

We've found that the physical properties of slags hinge on the interaction between polymerization processes and their phase makeup:

- at a basicity level of 1.0, chromium oxide acts in a way that simplifies the slag's structure, resulting in a bridging oxygen (BO) value of 0.55. This simple structure leads to a low viscosity of $0.25 \text{ Pa}\cdot\text{s}$ at the temperature where crystallization starts, which is 1530°C , even though there's a high presence of high-temperature phases;

- on the contrary, when the basicity reaches 2.5, the degree of polymerization in the slag increases ($\text{BO} = 0.73$). This is because Cr_2O_3 starts to show acidic properties, as seen by the formation of the $[\text{CrO}_4]$ structural unit in the slag. Along with this, there's a significant increase in high-temperature phases, by about 1.57 times. This combination leads to a more complex structure, pushing the slag's viscosity up to $1.0 \text{ Pa}\cdot\text{s}$ at 1670°C and raising the temperature at which crystallization begins to 1700°C .

REFERENCES / СПИСОК ЛИТЕРАТУРЫ

1. Kalicka Z., Kawecka-Cebula E., Pytel K. Application of the Iida model for estimation of slag viscosity for $\text{Al}_2\text{O}_3 - \text{Cr}_2\text{O}_3 - \text{CaO} - \text{CaF}_2$. *Archives of Metallurgy and Materials*. 2009;54(1):179–187.
2. Dyudkin D.A., Kisilenko V.V. *Production of Steel. In 3 vols. Vol. 3. Extra-Furnace Metallurgy of Steel*. Moscow: Teplotekhnika; 2010:544. (In Russ.).
- Дюдкин Д.А., Кисиленко В.В. *Производство стали. В 3-х томах. Т. 3. Внепечная металлургия стали*. Москва: Технопромиздат; 2010:544.
3. Wang H.M., Li G.R., Li B., Zhang X.J., Yan Y.Q. Effect of B_2O_3 on melting temperature of cao-based ladle refining slag. *Journal of Iron and Steel Research International*. 2010;17(10):18–22.
[https://doi.org/10.1016/S1006-706X\(10\)60177-X](https://doi.org/10.1016/S1006-706X(10)60177-X)
4. Wang H.M., Zhang T.W., Zhu H., Yan Y.Q., Zhao Y.N. Effect of B_2O_3 and CaF_2 on viscosity of ladle refining slag. *Advanced Materials Research*. 2011;295–297:2647.
<https://doi.org/10.4028/www.scientific.net/AMR.295-297.2647>
5. Babenko A.A., Shartdinov R.R., Upolovnikova A.G., Smetannikov A.N., Gulyakov V.S. Physical properties of slags of $\text{CaO} - \text{SiO}_2 - \text{B}_2\text{O}_3$ system containing 15 % of Al_2O_3 and 8 % of MgO . *Izvestiya. Ferrous Metallurgy*. 2019;62(10):769–773. (In Russ.).
<https://doi.org/10.17073/0368-0797-2019-10-769-773>
- Бабенко А.А., Шартдинов Р.Р., Уполовникова А.Г., Сметанников А.Н., Гуляков В.С. Физические свойства шлаков системы $\text{CaO} - \text{SiO}_2 - \text{B}_2\text{O}_3$, содержащей 15 % Al_2O_3 и 8 % MgO . *Известия вузов. Черная металлургия*. 2019;62(10):769–773.
<https://doi.org/10.17073/0368-0797-2019-10-769-773>
6. Tokovoi O.K. *Argon-Oxygen Refining of Stainless Steel*. Chelyabinsk: South Ural State University; 2015:250. (In Russ.).
- Токовой О.К. *Аргонокислородное рафинирование нержавеющей стали*. Челябинск: ИЦ ЮУрГУ; 2015:250.
7. Shtengel'meier S.V., Prusov V.A., Bogachev V.A. Improvement of the viscosity measurement technique with a vibrating viscometer. *Zavodskaya laboratoriya*. 1985;51(9):56–57. (In Russ.).
- Штенгельмайер С.В., Прусов В.А., Богачев В.А. Усовершенствование методики измерения вязкости вибрационным вискозиметром. *Заводская лаборатория*. 1985;51(9):56–57.
8. Voskoboinikov V.G., Dunaev N.E., Mikhalevich A.G., Kukhtin T.I., Shtengel'meier S.V. *Properties of Liquid Blast Furnace Slags*. Moscow: Metallurgiya; 1975:180. (In Russ.).
- Воскобойников В.Г., Дунаев Н.Е., Михалевич А.Г., Кухтин Т.И., Штенгельмайер С.В. *Свойства жидких доменных шлаков*. Москва: Металлургия; 1975:180.
9. Roine A. *HSC 6.0 Chemistry Reactions and Equilibrium Software with Extensive Thermochemical Database and Flowshut*. Pori: Outokumpu Research Oy; 2006:448.
10. Böcker J. *Spektroskopie: Instrumentelle Analytik mit Atom- und Molekülspektrometrie*. Würzburg: Vogel Communications Group GmbH & Co. KG; 1997:519. (In Germ.).
- Бёккер Ю. *Спектроскопия / Пер. Л.Н. Казанцева*. Москва: РИЦ Техносфера, 2009:528.
11. McMillan P. Structural studies of silicate glasses and melts—applications and limitations of Raman spectroscopy. *American Mineralogist*. 1984;69(6):622–644.
12. Matson D.W., Sharma S.K., Philpotts J.A. The structure of high-silica alkali-silicate glasses. A Raman spectroscopic investigation. *Journal of Non-Crystalline Solids*. 1983;58(2–3): 323–352. [https://doi.org/10.1016/0022-3093\(83\)90032-7](https://doi.org/10.1016/0022-3093(83)90032-7)
13. McMillan P.F., Poe B.T., Gillet P.H., Reynard B. A study of SiO_2 glass and supercooled liquid to 1950 K via high-temperature Raman spectroscopy. *Geochimica et Cosmochimica Acta*. 2001;58(17):3653–3662.
[https://doi.org/10.1016/0016-7037\(94\)90156-2](https://doi.org/10.1016/0016-7037(94)90156-2)
14. Kim T.S., Park J.H. Structure-viscosity relationship of low-silica calcium aluminosilicate melts. *ISIJ International*. 2014;54(9):2031–2038.
<https://doi.org/10.2355/isijinternational.54.2031>
15. Dines T.J., Inglis S. Raman spectroscopic study of supported chromium (VI) oxide catalysts. *Physical Chemistry Chemical Physics*. 2003;5(6):1320–1328.
<https://doi.org/10.1039/b211857b>
16. Weckhuysen B.M., Wachs I.F. Raman spectroscopy of supported chromium oxide catalysts. Determination of chromium–oxygen bond distances and bond orders. *Journal of the Chemical Society, Faraday Transactions*. 1996;92(11): 1969–1973. <https://doi.org/10.1039/FT9969201969>
17. Kim Y., Morita K. Relationship between molten oxide structure and thermal conductivity in the $\text{CaO}-\text{SiO}_2-\text{B}_2\text{O}_3$ system. *ISIJ International*. 2014;54(9):2077–2083.
<https://doi.org/10.2355/isijinternational.54.2077>
18. Cochaint B., Neuville D.R., Henderson G.S., McCammon C.A., Pinet O., Richet P. Effects of the iron content and redox state on the structure of sodium borosilicate glasses: A Raman, Mössbauer and boron K-Edge XANES spectroscopy study. *Journal of the American Ceramic Society*. 2012;95(3):962–971.
<https://doi.org/10.1111/j.1551-2916.2011.05020.x>
19. Li Q., Gao J., Zhang Y., An Z., Guo Z. Viscosity measurement and structure analysis of Cr_2O_3 -bearing $\text{CaO}-\text{SiO}_2-\text{MgO}-\text{Al}_2\text{O}_3$ slags. *Metallurgical and Materials Transactions B*. 2017;48:346–356.
<https://doi.org/10.1007/s11663-016-0858-8>

20. Xu R.Z., Zhang J.L., Wang Z.Y., Jiao K.X. Influence of Cr_2O_3 and B_2O_3 on viscosity and structure of high alumina slag. *Steel Research International*. 2017;88(4):1600241. <https://doi.org/10.1002/srin.201600241>
21. Sun Y., Zhang Z. Structural roles of boron and silicon in the $\text{CaO}-\text{SiO}_2-\text{B}_2\text{O}_3$ glasses using FTIR, Raman, and NMR spectroscopy. *Metallurgical and Materials Transactions B*. 2015;46:1549–1554. <https://doi.org/10.1007/s11663-015-0374-2>
22. Cai Z., Song B., Li L., Liu Zh., Cui X. Effects of B_2O_3 on viscosity, structure, and crystallization of mold fluxes for casting rare earth alloyed steels. *Metals*. 2018;8(10):737. <https://doi.org/doi:10.3390/met8100737>
23. Mysen B.O., Virgo D., Scarfe C.M. Relations between the anionic structure and viscosity of silicate melts – a Raman spectroscopic study. *American Mineralogist*. 1980;65(7):690–710.
24. Forsbacka L., Holappa L., Kondratiev A., Jak E. Experimental study and modelling of viscosity of chromium containing slags. *Steel Research International*. 2007;78(9):676–684. <http://dx.doi.org/10.1002/srin.200706269>
25. Wu T., Zhang Y., Yuan F., An Z. Effects of the Cr_2O_3 content on the viscosity of $\text{CaO}-\text{SiO}_2-10 \text{ Pct } \text{Al}_2\text{O}_3-\text{Cr}_2\text{O}_3$ quaternary slag. *Metallurgical and Materials Transactions B*. 2018;49:1719–1731. <https://doi.org/10.1007/s11663-018-1258-z>

Information about the Authors

Anatolii A. Babenko, Dr. Sci. (Eng.), Prof., Chief Researcher, Institute of Metallurgy, Ural Branch of the Russian Academy of Sciences
ORCID: 0000-0003-0734-6162
E-mail: babenko251@gmail.com

Ruslan R. Shartdinov, Junior Researcher of the Laboratory of Steel and Ferroalloys, Institute of Metallurgy, Ural Branch of the Russian Academy of Sciences
ORCID: 0000-0003-0852-1161
E-mail: rr.shartdinov@gmail.com

Alena G. Upolovnikova, Cand. Sci. (Eng.), Senior Researcher of the Laboratory of Steel and Ferroalloys, Institute of Metallurgy, Ural Branch of the Russian Academy of Sciences
ORCID: 0000-0002-6698-5565
E-mail: upol.ru@mail.ru

Artem N. Smetannikov, Junior Researcher of the Laboratory of Steel and Ferroalloys, Institute of Metallurgy, Ural Branch of the Russian Academy of Sciences
ORCID: 0000-0001-9206-0905
E-mail: artem.smetannikov.89@mail.ru

Daniil A. Lobanov, Cand. Sci. (Eng.), Research Associate, Institute of Metallurgy Ural Branch of the Russian Academy of Sciences
ORCID: 0009-0007-5659-1208
E-mail: summerdanny@yandex.ru

Aleksei V. Dolmatov, Cand. Sci. (Chem.), Senior Researcher of the Laboratory of Metallurgical Melts, Institute of Metallurgy, Ural Branch of the Russian Academy of Science
ORCID: 0000-0002-6632-9533
E-mail: dolmatov.imet@gmail.com

Сведения об авторах

Анатолий Алексеевич Бабенко, д.т.н., профессор, главный научный сотрудник, Институт metallurgии Уральского отделения РАН
ORCID: 0000-0003-0734-6162
E-mail: babenko251@gmail.com

Руслан Рафикович Шартдинов, младший научный сотрудник лаборатории стали и ферросплавов, Институт metallurgии Уральского отделения РАН
ORCID: 0000-0003-0852-1161
E-mail: rr.shartdinov@gmail.com

Алена Геннадьевна Уполовникова, к.т.н., старший научный сотрудник лаборатории стали и ферросплавов, Институт metallurgии Уральского отделения РАН
ORCID: 0000-0002-6698-5565
E-mail: upol.ru@mail.ru

Артем Николаевич Сметаников, младший научный сотрудник лаборатории стали и ферросплавов, Институт metallurgии Уральского отделения РАН
ORCID: 0000-0001-9206-0905
E-mail: artem.smetannikov.89@mail.ru

Даниил Андреевич Лобанов, к.т.н., научный сотрудник, Институт metallurgии Уральского отделения РАН
ORCID: 0009-0007-5659-1208
E-mail: summerdanny@yandex.ru

Алексей Владимирович Долматов, к.х.н., старший научный сотрудник лаборатории metallургических расплавов, Институт metallurgии Уральского отделения РАН
ORCID: 0000-0002-6632-9533
E-mail: dolmatov.imet@gmail.com

Contribution of the Authors

A. A. Babenko – scientific guidance, data analysis, writing and editing the text.

R. R. Shartdinov – conducting the experiment, data processing and analysis, writing and editing the text.

A. G. Upolovnikova – modeling, data analysis, editing the text.

A. N. Smetannikov – conducting the experiment, data analysis.

D. A. Lobanov – conducting the experiment, data analysis.

A. V. Dolmatov – data processing and analysis.

Вклад авторов

А. А. Бабенко – руководство, анализ результатов, написание статьи, редактирование статьи.

Р. Р. Шартдинов – проведение эксперимента, обработка и анализ результатов, написание статьи, редактирование статьи.

А. Г. Уполовникова – моделирование, анализ результатов, редактирование статьи.

А. Н. Сметаников – проведение эксперимента, анализ результатов.

Д. А. Лобанов – проведение эксперимента, анализ результатов.

А. В. Долматов – обработка и анализ результатов.

Received 14.04.2023

Revised 06.07.2023

Accepted 11.09.2023

Поступила в редакцию 14.04.2023

После доработки 06.07.2023

Принята к публикации 11.09.2023